



Review

# A Review on the Effects of Organic Structure-Directing Agents on the Hydrothermal Synthesis and Physicochemical Properties of Zeolites

Zahra Asgar Pour  and Khaled O. Sebakhy \* 

Department of Chemical Engineering, Engineering and Technology Institute Groningen (ENTEG), University of Groningen, Nijenborgh 4, 9747 AG Groningen, The Netherlands; z.asgar.pour@rug.nl

\* Correspondence: k.o.sebakhy@rug.nl; Tel.: +31-(0)6-2992-8542

**Abstract:** The study on the synthesis of zeolites, including both the development of novel techniques of synthesis and the discovery of new zeolitic frameworks, has a background of several decades. In this context, the application of organic structure-directing agents (SDAs) is one of the key factors having an important role in the formation of porous zeolitic networks as well as the crystallization process of zeolites. There are various elements that are needed to be explored for elucidating the effects of organic SDAs on the final physicochemical properties of zeolites. Although SDAs were firstly used as pore generators in the synthesis of high-silica zeolites, further studies proved their multiple roles during the synthesis of zeolites, such as their influences on the crystallization evolution of zeolite, the size of the crystal and the chemical composition, which is beyond their porogen properties. The aim of this mini review is to present and briefly summarize these features as well as the advances in the synthesis of new SDAs during the last decades.

**Keywords:** structure directing agents; templating methods; co-templating methods; organic templates; inorganic templates; zeolite crystal size; zeolite Si/Al ratio; dual-templating; SDAs; pore-filling agents



**Citation:** Asgar Pour, Z.; Sebakhy, K.O. A Review on the Effects of Organic Structure-Directing Agents on the Hydrothermal Synthesis and Physicochemical Properties of Zeolites. *Chemistry* **2022**, *4*, 431–446. <https://doi.org/10.3390/chemistry4020032>

Academic Editors: Mathias S. Wickleder and Catherine Housecroft

Received: 18 March 2022

Accepted: 9 May 2022

Published: 13 May 2022

**Publisher's Note:** MDPI stays neutral with regard to jurisdictional claims in published maps and institutional affiliations.



**Copyright:** © 2022 by the authors. Licensee MDPI, Basel, Switzerland. This article is an open access article distributed under the terms and conditions of the Creative Commons Attribution (CC BY) license (<https://creativecommons.org/licenses/by/4.0/>).

## 1. Introduction

Zeolites with both natural and synthetic origins are metallosilicate materials possessing unique physicochemical properties such as crystallinity, acidity, hydrothermal stability, ion-exchange ability and shape selectivity [1,2]. Due to these prominent features, zeolites are applicable in different commercial fields such as catalysis, adsorption and separation processes [3–5]. On the other hand, their synthesis is a challenging task that requires the tuning of several parameters in order to obtain the desired product at the end of the process. For instance, chemical compositions of precursors, type of mineralizers, temperature, aging time as well as the type and concentration of structure-directing agents (SDAs) are needed to be optimized smartly during the synthesis of zeolites [6,7]. From the historical background, for both lab and commercial synthesis of zeolites, great strides have been made in the twentieth century, which began with the pioneering works of Barrer [8]. However, from the time of the discovery of natural zeolites dating back to the eighteenth century, mineralogists and chemists put a lot of effort into disclosing how zeolites are formed in nature. From the mid-20th century, several zeolites with different topologies (e.g., MOR, FAU, MFI and BEA frameworks) were obtained in the lab. All these zeolites have natural analogs known before or in some cases after the synthesis in the lab [9]. Despite the topological similarities between these two classes of zeolites, an obvious distinction is the absence of organic structure-directing agents (SDAs) in the process of formation of natural zeolites [9]. Interestingly, the first generation of lab-made zeolites (e.g., LTA and FAU topologies, also characterized as low Si/Al zeolites) were synthesized in the absence of organic SDAs and entirely by the aid of inorganic precursors in which the alkali and alkali

earth metals performed the role of SDAs [10,11]. Thereafter, utilizing the organic SDAs proved to be a method for the synthesis of new zeolitic frameworks with higher Si/Al ratios, such as ZSM-5 (MFI) and zeolite Beta (BEA), and also assist in the facile synthesis of other zeolites such as FAU and LTA frameworks, which were previously prepared in the absence of organic SDAs [12–14]. In this context, simple organic molecules such as quaternary ammonium molecules or small amines were the first generation of organic SDAs [15]. The application of these molecules in the synthesis of zeolites was a turning point for the future research directed in the field of synthesis of new SDAs in order to discover new zeolitic structures such as several high Si/Al ratio frameworks or odd-member ring frameworks having 11- or 15-T atom rings in their structure [16–18]. Here, the T atom is representative of Si or other framework heteroatoms such as Al, B, Ga, Ge and so forth. To attain this goal, various properties of the final SDAs such as geometrical properties, hydrophobicity and structural stability should be addressed properly [19,20]. In addition, other factors such as the affinity between SDA molecules themselves, the interaction between SDA molecules and zeolite precursors and the location of SDA within the zeolite porous network (e.g., inside channels or cages) govern how the zeolite crystallization evolves [21,22]. From this standpoint, an overview of different organic species used in zeolite synthesis seems essential. On the subject of organic SDAs, the type of interaction that leads to crystallization is very important. A simple but conceptual definition is that organic SDA species cause the crystallization of microporous zeolites, while some other organic molecules, which cannot themselves nurture the crystallization process of zeolites, are categorized as pore-fillers [23]. They can be added to the zeolite primary suspension containing the SDA to merely occlude the pores and thus they have no effect on the formation of zeolite structures as well as the crystallization step [23–28]. In view of functionality, pore-filling agents can be also served in the case of the treatment of as-synthesized zeolites, in order to occupy zeolite pores and to prevent the destruction of pores or dissolution of pore constituent elements in the acidic or basic medium [24]. They can also be used in the formation of multi-dimensional pore systems where the stabilization of one type of channel or cavity requires the utilization of additional organic moieties, which does not exactly act like SDA species [25]. In other words, the presence of pore-fillers is not solely enough for zeolite crystallization and besides that, the molecule should have the ability of structuring and stabilizing the pores to be considered as an SDA molecule [26–29]. In short, the functionality of organic SDAs is notably different from pore-filling agents and the organic SDA also plays the role of a pore-filling agent, while pore-filling agents cannot necessarily play the role of organic SDAs and are less- or non-selective to the zeolitic phase formation but provide enough basicity for zeolite formation [28,30,31]. For reasons of transparency, the term true template has been used as a similar or equivalent term to SDAs in many studies [27–33]. Despite several similarities, true templates are also applied for the synthesis of zeolitic frameworks that are synthesized only by means of a limited number of SDAs or a single type of SDA [34]. In this respect, a few organic species are available as true templates, but they are still SDAs and their functionality does not differ from SDAs [34–36]. The term modifier in zeolite synthesis is applied when an additive is used to alter the interactions, for example, with zeolite Al species [37] or orienting zeolite films on a surface, which is called a surface modifier, such as organic surfactants [38]. However, the aim of this review is to illuminate exclusively the role of organic SDAs in the synthesis of zeolites, which indubitably have a structuring role during the crystallization process.

It is noteworthy that the chemical properties of zeolites including both the number of active sites (e.g., Al atoms) as well as their location in the framework are affected by the type of SDA so that the application of different SDAs leads to different catalytic properties for a given synthesized zeolite [39]. Another reason to investigate new SDA materials was the microporous nature of conventional zeolites (with pore diameter < 2 nm), which is a limiting factor for their application in catalyzing bulky molecules (e.g., biobased compounds reactions in liquid phase). In this regard, the synthesis of large-pore zeolites having 14-T, 18-T, 20-T 28-T and 30-T atoms in one ring is one of the strategies for solving diffusion

limitations inside the micropores [15,40,41]. Another strategy is the synthesis of so-called “hierarchical zeolites” possessing secondary mesopores ( $2 \text{ nm} < dp < 50 \text{ nm}$ ) as well as macropores ( $dp > 50 \text{ nm}$ ) along with the original micropores using new SDAs [42]. The former class of zeolite was mainly synthesized by means of soft templating techniques. An interesting example is the synthesis of mesoporous Engelhard titanosilicates (known as titanosilicates possessing both octahedral  $\text{TiO}_6$  and tetrahedral  $\text{SiO}_4$  in their structure) in the presence of cetyltrimethylammonium bromide ( $\text{C}_{16}\text{TMAB}$ ) or other tetraalkyl bromides, which remarkably change the size and morphology crystals of these zeolites [43,44]. On the other hand, obtaining hierarchical zeolites has been achieved by the application of both soft and hard templating techniques, and here the former one is a matter of discussion [45,46]. For the sake of clarity, the hard templating technique is also used for macroscopic shaping of zeolites using several macroscopic solid templates (e.g., polymeric beads [47], carbon monoliths [48], organic aerogels [49], and polyurethane foams [50]), which is beyond the scope of this review. It is noteworthy to mention that zeolites can be directly synthesized from raw materials (e.g., mineral clays) or industrial waste (e.g., fly ash) by means of hydrothermal transformation with a wide range of applications in adsorption and separation processes. Although this synthetic protocol is not in the scope of our review, it is a very useful technique that can diminish the negative impacts of industrial wastes on the environment [51–53]. In addition, the incorporation of heteroatoms in a metal–zeolite framework (e.g., Ni-MFI topology) rather than conventional Al-containing zeolites needs the synthesis technique, which is modified by altering pH and the type of precursors as the interaction of heteroatoms with organic SDA can differ from Al and Si [54].

The aim of this review is to provide a survey about the role and effects of SDAs in the synthesis of zeolites, as well as the recent advances in the field of the synthesis of novel SDAs. The effect of SDAs on zeolite physicochemical properties (e.g., Si/Al ratio, acidity, textural properties and crystal growth) is demonstrated in Figure 1 and further discussed in the following sections of this review.

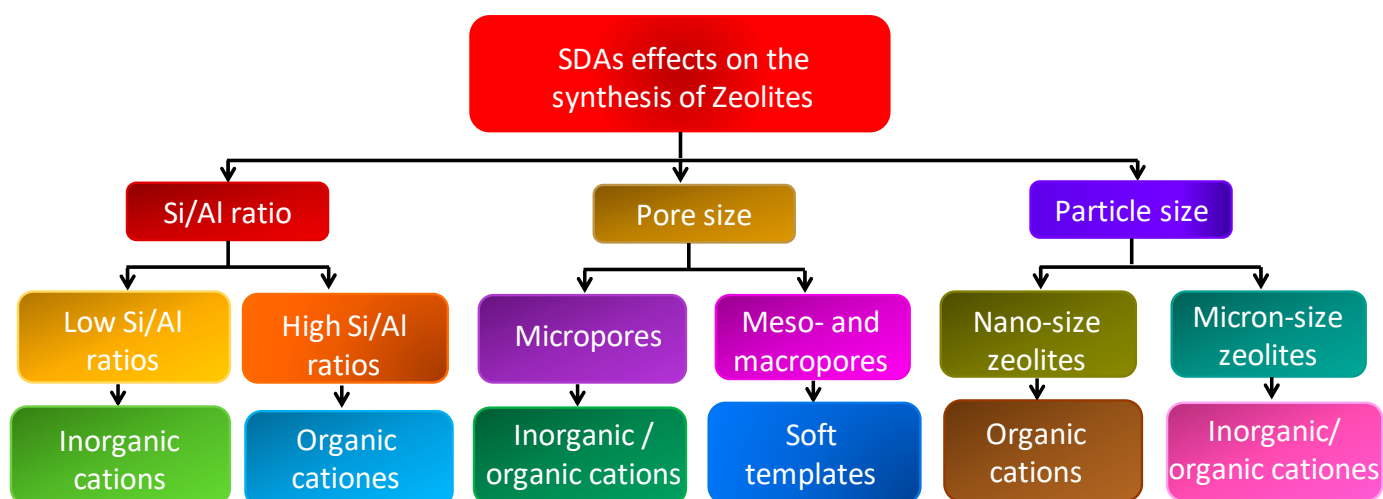


**Figure 1.** The effects of SDAs on the physicochemical properties of zeolites.

## 2. Effects of SDAs on the Chemical Composition of Zeolites (or Si/Al Ratio)

SDAs were firstly employed to obtain new zeolites with higher Si/Al ratios (e.g.,  $\text{SiO}_2/\text{Al}_2\text{O}_3 > 5$ ) and for this purpose, molecules such as quaternary ammonium were used [12,13,55,56]. As stated before, in the first generation of zeolites with low Si/Al ratios ( $\text{Si}/\text{Al} < 3$ ), micropores were produced by trapping inorganic cations (e.g.,  $\text{Na}^+$ ,  $\text{K}^+$ ) within the zeolite precursors, which are forming the zeolite primary building blocks. The structural rearrangement of zeolite primary building blocks around these cations led to the formation of final zeolite product after crystallization completion. Inorganic cations, stabilize the zeolitic framework by neutralizing the lattice charges. Although the

presence of inorganic and organic SDAs has also shown to have cooperative effects on the crystallization process of zeolites [57], the presence of organic SDAs is essential in the case of the synthesis of zeolites with higher Si/Al ratios to fill the pores, prevent the dissolution of precursors and meanwhile stabilize the porous structure as well (see Figure 2) [58]. For example, in the case of LTA-type zeolites, with the assistance of tetramethylammonium cations ( $\text{TMA}^+$ ) and  $\text{Na}^+$ , the Si/Al ratio of the zeolite was increased from 1 to 3, indicating that the number of tetrahedrally coordinated Al atoms will decrease in the presence of  $\text{TMA}^+$  [59]. Following this, using a mixture of  $\text{TMA}^+$  and larger tetraethylammonium cations ( $\text{TEA}^+$ ), the Si/Al ratio of LTA zeolite increased to 9 (zeolite UZM-9) [59]. The impact of organic SDAs on the chemical composition of zeolite has been more elucidated when the pure silica and highly hydrophobic LTA (ITQ-29, Si/Al =  $\infty$ ) was synthesized using a supramolecular SDA [60]. Although some zeolites with high Si/Al ratios can be also prepared solely in the presence of inorganic cations, notable amounts of seeds are used for this aim (so-called “seeding technique”), which is not the target of this study [61]. The role of organic SDAs in lowering the amount of Al atoms is attributed to their larger size and the lower amounts of positive charges that they insert in the lattice compared to the number of charges introduced by small inorganic cations. Accordingly, lower negative charges are required for neutralization of the lattice charge, which rationalizes the contribution of lower Al atoms in the structure [62,63]. This finding was helpful for the facile synthesis of high-silica zeolites (Si/Al > 10) with high hydrothermal stability and strong Brønsted acidity as suitable heterogeneous catalysts for utilization in gas phase reactions at elevated temperatures in which the strong type of Brønsted acidity is generated due to the presence of lower population of Al atoms in the framework [62].

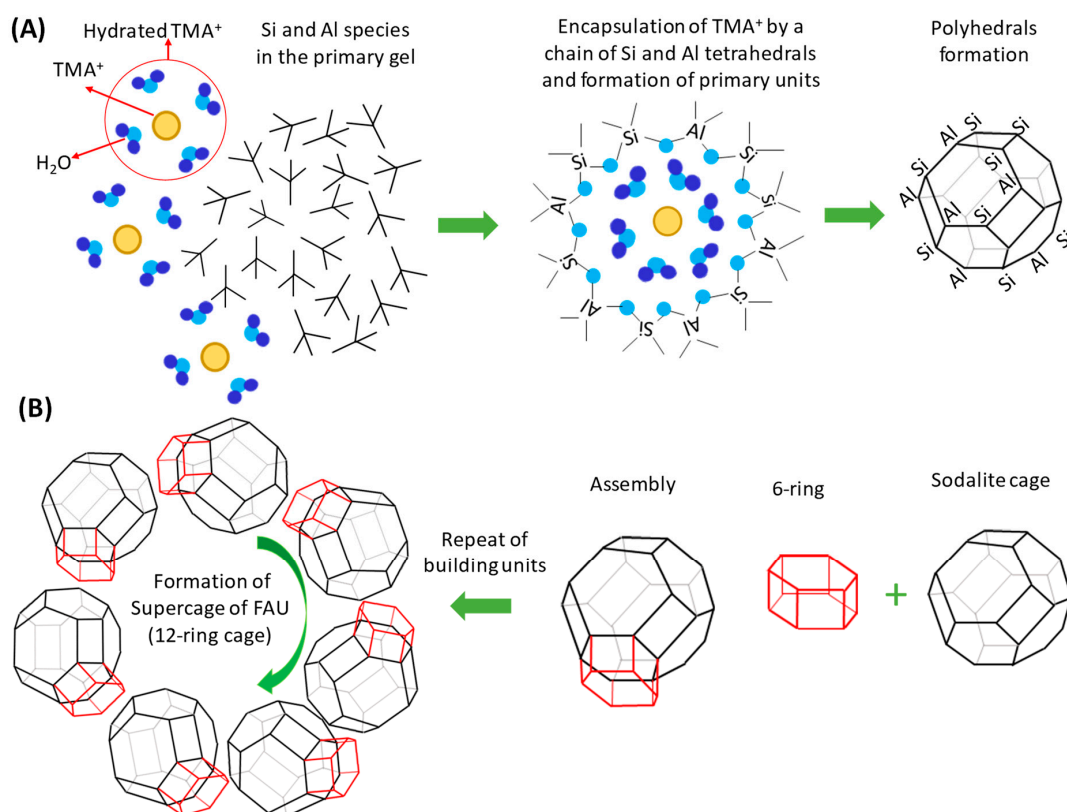


**Figure 2.** Schematic representation of (A) The formation of primary zeolitic Y building blocks (FAU topology) around organic SDAs ( $\text{TMA}^+$ ) and (B) the formation of zeolite Y supercage by assembly of secondary building blocks (i.e., sodalite and 6-ring units).

It should be noticed that the use of SDAs is not limited to one topology and several frameworks are synthesized using different concentrations of the same SDA. Here, the

composition of primary gel also affects the selectivity of zeolite phase (see Table 1). For example, the presence of higher amounts of heteroatoms such as Al in the primary gel (e.g., Si/Al molar ratio of ~ 10–20) conducts the formation of open zeolitic frameworks with low framework densities, which is accomplished by promoting the formation of higher numbers of 4-ring (4 dr) building blocks [64]. In addition to the experimental works that have been performed on the effect of SDA on the Si/Al ratio of zeolite, after the 1990s, by development and application of computational techniques and advanced theories of quantum mechanics (e.g., Density Functional Theory, DFT), scientists are trying to predict the location and type of active sites (e.g., Al) as well as the structure of hypothetical zeolites using new SDAs in advance [18,65,66]. Computational techniques in many cases have been helpful for interpretation of the mechanism of cooperation of SDAs with the negative framework species. Accordingly, Al distribution and position can be explored based on the SDA occupancy within the zeolite void spaces [63,67,68]. The effect of SDA on altering the final Si/Al ratio of zeolite is shown in Table 1.

**Table 1.** Effects of organic SDAs on the Si/Al ratio of synthesized zeolites [69,70].

Entry	Zeolite Topology	Zeolite Name	Obtained Si/Al	SDA
1	CHA	Chabazite	2.1	No SDA
		SSZ-13	13.3	N,N,N-trimethyl-1-adamantammonium
2	EDI	Linde Type F	1.0	No SDA
			1.5	TMA <sup>+</sup>
3	EMT	EMC-2	1.1	No SDA
			3.8	crown ether
4	FAU	Linde Type Y	2.4	No SDA
		High Si EMC-1	3.8	15-crown-5
5	KFI	ZK-5	3.4	No SDA
		High Silica KFI	3.8	18-crown-6
6	LTA	Linde Type A	1.0	No SDA
		ZK-4	1.4	TMA <sup>+</sup>
7	OFF	Zeolite Alpha	3.0	TMA <sup>+</sup>
		Linde Type T	3.5	No SDA
		Offretite	3.8	TMA <sup>+</sup>

### 3. Effects of SDAs on the Zeolite Crystallization Process

SDAs with insufficient hydrophobicity display low interaction with inorganic moieties, which affects the crystallization step by promoting the formation of competitive amorphous phases [71]. Such an effect was observed in our experiments when we were trying to synthesize spherically shaped zeolite Y (i.e., in bead form) using a type of macroscopic polymeric beads as the shaping template. Compared with zeolite primary gel, the polymeric beads have different chemical compositions and surface chemistry, which is more likely arising from the presence of functionalized groups attached to their surface. For that reason, the crystallization around these polymeric beads was not successful compared to the bulk of zeolite (i.e., in powder form). Obviously, better crystallinity was obtained for zeolite Y beads using TMA<sup>+</sup> compared to the non-organic templating synthesis (see Figure 3). The size of crystallites of both zeolite Y samples was calculated based on Scherrer equation and the results showed an average crystallite size of 43.28 nm in the case of zeolites synthesized in the presence of TMA<sup>+</sup> and 84.05 nm in the sample synthesized in the absence of TMA<sup>+</sup>.

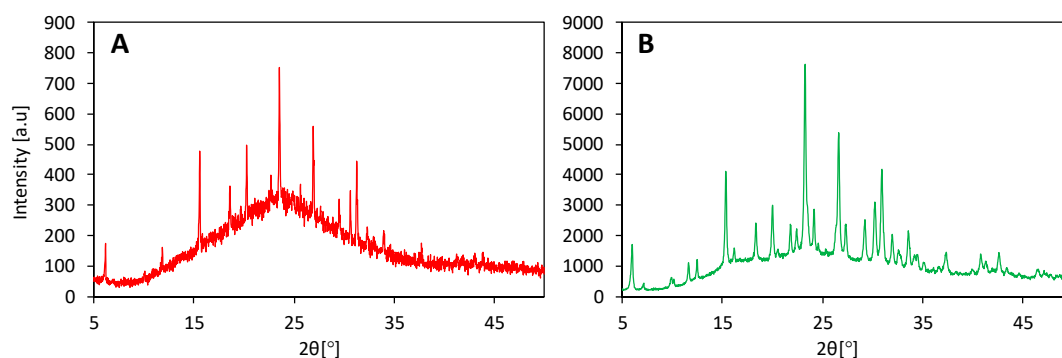


**Figure 3.** Diffractogram of (A) Zeolite Y beads prepared in our lab in the absence of organic SDA and (B) Zeolite Y beads prepared in our lab in the presence of TMA<sup>+</sup>.

In addition, the particle size visualized by SEM techniques is not shown here and reflected that the presence of TMA<sup>+</sup> as SDA notably increases the size of zeolite Y particles (from the average size of 3.5  $\mu$  in the absence of SDA to an average size of 74  $\mu$  in the presence of TMA<sup>+</sup>). However, it should be noticed that due to the semi-amorphous nature of the zeolite Y spheres prepared in the absence of TMA<sup>+</sup>, the size of the particles visualized by SEM is approximately measured (in some parts, amorphous phases covered the surface of particles). Such observations are pointing out that SDAs are not only working as pore-fillers but also interact with the Si species mainly through van der Waals forces [72]. It also demonstrates that SDAs can determine the geometry of zeolite pores and the type of final crystalline structure [73].

Nonetheless, the comprehension of how micropores are generated by the aid of SDA molecules and how crystallization propagates within the primary gel is still a matter of argument [74]. It is known that the type of interaction between zeolite precursors and SDAs can alter the concentration of the organic template in the zeolite framework. In other words, the total energy of a zeolite–SDA system is lower in a framework with densely-packed SDAs [72,73]. Moreover, the more possibly formed structures during the crystallization of zeolites by employing SDAs are not the most stable ones but are those ones with the greatest nucleation abilities growing under thermodynamic or kinetic control. This phenomenon depends on the conditions of crystals' growth step during the crystallization process [39]. Finally, other factors such as amounts of trivalent atoms (e.g., Al), presence of other heteroatoms such as germanium, the H<sub>2</sub>O/Si molar ratio and the type of mineralizers (e.g., OH<sup>-</sup>, F<sup>-</sup>) can influence the formation of certain crystalline structures. These factors become more pronounced if the SDA species are not fully matched within the porous network of a certain zeolitic structure [75,76]. For instance, gallosilicate ECR-34 with ETR topology (18-T atoms in one ring) is synthesized via collaboration between organic SDA and two inorganic cations (See Figure 4). For the synthesis of this material, TEA<sup>+</sup>, Na<sup>+</sup> and K<sup>+</sup> are utilized for structuring the porous network [77].

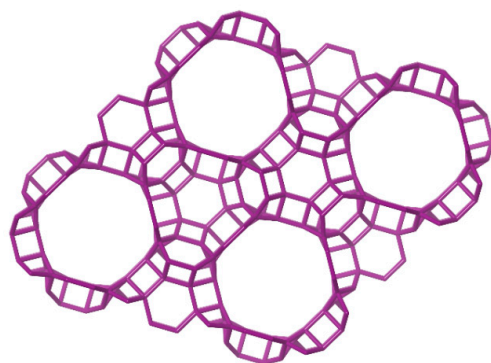


**Figure 4.** ETR framework overview containing large cages with ring size of 18-T atoms; (the image is produced by 3D drawing tool in database of zeolites structures, Accessed 17 March 2022) [78].

#### 4. Application of the SDAs in the Formation of Microporous Zeolites

The relation between the size and geometry of SDA molecules and the final configuration of generated cavities is attributed to the interactions between the SDA and inorganic framework of zeolites, by which the rotation of SDA inside a forming pore is prohibited by negatively charged species [79]. In this regard, small and spherical molecules can form Clathrasils possessing polyhedral cavities with small windows, which are not large enough for bulky molecules to pass through them easily [80]. Larger branched molecules such as quaternary ammonium molecules (e.g., TMA<sup>+</sup>, TEA<sup>+</sup>, etc.) possess rigid structures and mainly generate 3D zeolites (e.g., MFI or BEA topology, Figure 5), while linear diquaternary cations such as hexamethonium cation are flexible species and generate 1D porous networks such as ZSM-48 and EU-1 (\* MRE and EUO framework, respectively) [81,82].

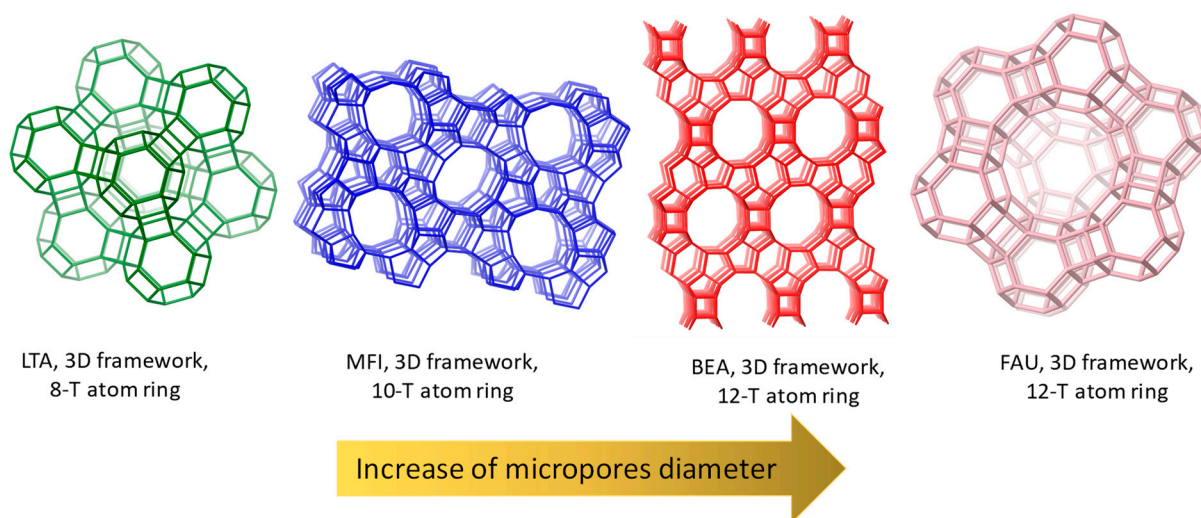


**Figure 5.** Microporous zeolites with different types of pores and channels, (images are produced by 3D drawing tool in database of zeolites structures, Accessed 17 March 2022) [78].

Afterwards, the next generation of SDAs was synthesized by modification of C-substituted piperidine through derivatization on the nitrogen atom to give primary, secondary and tertiary amines. By using these SDAs, various types of high-silica zeolites such as SSZ-23, SSZ-35, SSZ-39 and SSZ-44 were synthesized [83]. In addition, by placing organic molecules at the end of the chain of linear diamines and using them as SDAs, several new structures such as IM-5, TNU-9, TNU-10, SSZ-74 and SSZ-75 were obtained [83–87]. The 1D pentasil zeolites with high Si/Al ratios such as ZSM-12 (MTW), ZSM-22 (TON) and ZSM-23 (MTT) were obtained using the derivative molecules synthesized by mono- or multiple alkylation of imidazole [88]. By conducting the synthesis in HF medium and using substituted imidazoles, ITQ-12 (ITW) was obtained [89]. SSZ-70 and IM-16 (UOS) were also synthesized using this SDA in the presence of boron and germanium, respectively [90,91]. For the synthesis of SIZ-7 (SIV) imidazolium was used as the SDA [92]. MFI zeolites, which are synthesized commonly in the presence of TPA<sup>+</sup> cations, have been also prepared using hydrothermally stable di- and triquaternary ammonium cations [29]. Other frameworks such as MOR, MTW, SSZ-31, SSZ-37 and MSE were prepared using SDAs obtained by Diels–Alder reaction [93,94]. In these cases, rigidity is an important factor for the selection of SDAs to produce low-density and highly porous frameworks with 3D and large pores such as CIT-1 (CON) or MCM-68 (MSE) topologies [95]. MCM-68 is the first zeolite synthesized with channels having 12-T atom rings [95]. Here, a very large and rigid SDA obtained by Diels–Alder reaction was used to produce such large channels [95]. SSZ-50 (RTH) was synthesized using polycyclic SDAs prepared by Beckmann rearrangement reaction [96]. SSZ-56 (SSF) was synthesized by employing a bicyclic SDA prepared by catalytic hydrogenation of substituted quinolone [97]. In addition, SSZ-55, SSZ-57 and SSZ-58 (SFG) were

synthesized by reductive amination of ketones [98,99]. SSZ-53, SSZ-59 (SFN) and SSZ-65 (SSF) were synthesized by the amination of acyl amine [100–102]. Despite the long list and diversity of the above-mentioned SDAs, their application also has some limitations originating from their higher hydrophobicity and large size, which are troublesome for their solubility in the aqueous medium and to generate solvated cations. Indeed, the carbon-to-nitrogen ratio of these species is an indication and the optimum range has been reported to be between  $11 < C/N^+ < 15$  to assist the formation of high-silica zeolites [58]. This demonstrates that a moderate hydrophobicity grants better ability to such SDA to efficiently crystallize high-silica zeolites [103]. In contrast, inherently hydrophilic SDAs can be generally inappropriate species due to the formation of hydration spheres around their structure, and therefore, these species hardly interact with  $SiO_4^-$  precursors [103].

### 5. Co-Templating Technique Using Organic SDAs

The idea of the co-templating technique originated from the synergic cooperation of two or more organic SDAs to generate different types of secondary building units (SBUs) in the final structure. Moreover, other species such as inorganic cations (e.g.,  $Na^+$ ),  $F^-$ , Ge and  $H_2O$  also have co-templating roles during the zeolite crystallization step. The co-templating effects of two or more organic SDAs in the formation of a specific zeolitic phase become more essential when cavities and channels with different diameters and geometries cannot be created merely using one organic SDA. In such cases, the application of at least two SDAs can facilitate the zeolite formation where each SDA builds up one of the porous network components (e.g., cages or channels). The distribution of framework heteroatoms (e.g., Al) and also their locations are directly influenced by the type and size of organic templates used in the co-templating technique. The heteroatoms are more likely placed in locations that are less accessible by SDAs [104,105]. A similar incorporation mechanism has been suggested for the insertion of Si atoms in SAPO materials prepared using co-templating techniques [30,31,106,107]. Co-templating also influences the crystallization process by altering nucleation and growth steps whereby the ultimate crystal size, morphology and chemical composition are directly affected by the presence of organic SDAs. As stated for mono-SDA application, the co-templating also increases the Si/Al ratio of final zeolite [108]. The formation of larger crystals, which has been frequently claimed in these cases, is directly linked to the low supersaturation rate in the zeolite primary suspension containing two or more templates, which can prevent the generation of large amounts of nucleation centers.

The first zeolite produced using the co-templating technique was ZSM-39 synthesized by combining  $TMA^+$  and propylamine and later by  $TMA^+$  and ethylamine as templates [109–111]. This zeolite consists of two different cavities with smaller pentagonal dodecahedron and larger hexadecahedron cages [111]. Further studies revealed that the formation of these cages depends on the SDA size, where larger  $TMA^+$  occupies the larger cavities and the propylamine fills the smaller cage. A primary zeo-type material synthesized using this technique is SAPO-37 (FAU) [112]. For the synthesis of this material, both  $TMA^+$  and  $TPA^+$  (tetrapropylammonium cation) are required as SDAs (Figure 6). In this case, a larger  $TPA^+$  is used to form larger FAU super cage while a smaller  $TMA^+$  is a suitable molecule for the formation of a smaller sodalite (sod) cage [113]. The  $TMA^+/TPA^+$  molar ratio is an important factor for the crystallization of SAPO-37, and beyond a narrow ratio, other phases such as SAPO-20 and SAPO-5 can be also formed [113].

SAPO-34 (CHA) is another example of zeo-type materials obtained also by the combination of  $TEA^+$  and di-n-propylamine or cyclohexylamine as the second SDA [114,115]. Alternatively, SAPO-34 has also been synthesized by triple-templating and employing  $TEA^+$ , trimethylamine and morpholine as organic SDAs, in which the ratio between these templates can significantly alter the physicochemical properties of SAPO-34 [116]. Other frameworks such as SSZ-25, SSZ-28, SSZ-32, SSZ-35, SSZ-47 and UZM-5 (UFI) have been synthesized using co-templating technique as well [117–119].



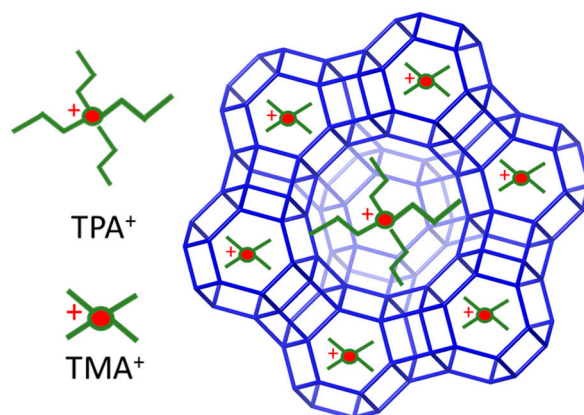


**Figure 6.** SAPO-37 synthesis using the co-templating technique: formation of the supercage using larger TPA<sup>+</sup> molecules and sodalite cage using smaller TMA<sup>+</sup> molecules (SAPO-37 image is produced by 3D drawing tool in database of zeolites structures, Accessed 17 March 2022) [78].

The co-templating technique is also beneficial for those zeolites that are synthesized using an expensive SDA. In this condition, the application of small quantities of an expensive SDA can initiate the nucleation, while the addition of more portions of inexpensive amines such as isopropyl- or isobutylamine enables the crystallization to move forward in a cost-effective direction. These amines efficiently occupy the pores (e.g., pore-filling agents) and stabilize them and meanwhile provide enough basicity to enhance the rate of crystallization of zeolites [120].

## 6. Soft-Templating Technique for the Synthesis of Large Pore and Hierarchical Zeolites

Applying bulky templates or so-called “soft templates” yields a network of interconnected pores with multi-level diameters also known as hierarchical zeolites. With respect to the presence of such porous systems, diffusion properties within the zeolite crystals can be improved. For instance, mesoporous zeolites have been synthesized using several types of soft templates, such as cationic surfactants, silylated polymers, cetyltrimethylammonium bromide, Pluronic F127 or a combination of these super large templates [121–123]. A hierarchical SAPO-34 structure was obtained by means of a quaternary ammonium-type organosilane surfactant and diethylamine [124]. The surfactant here was used as a mesopore generator and also as a part of silica precursor. This material displayed a nanosheet structure [124]. Moreover, a layered type of ZSM-5 has been prepared using a type of bulky SDA, consisting of two quaternary ammonium groups attached to the ends of a long-chain alkyl group with 22 carbons in a chain [125]. The cationic group acts as an SDA, while the hydrophobic chain prevents the particles from growing in the “b” direction, and so the zeolitic monolayers are produced in this protocol [125].

Finally, it would be interesting that the self-organization of surfactant molecules enables them to form supermolecular micelles, which can be also used as SDA for large pore formation (Figure 7). These species are intrinsically flexible and by smart design of their geometrical packing properties as well as their functional groups, better control on the porous structure is possible [126,127]. The application of co-surfactants, swelling agents and inorganic salts also increase the degree of control on geometrical packing of the micelle. However, the downside of this technique is in the formation of amorphous phases in addition to the crystalline zeolitic phase [128].

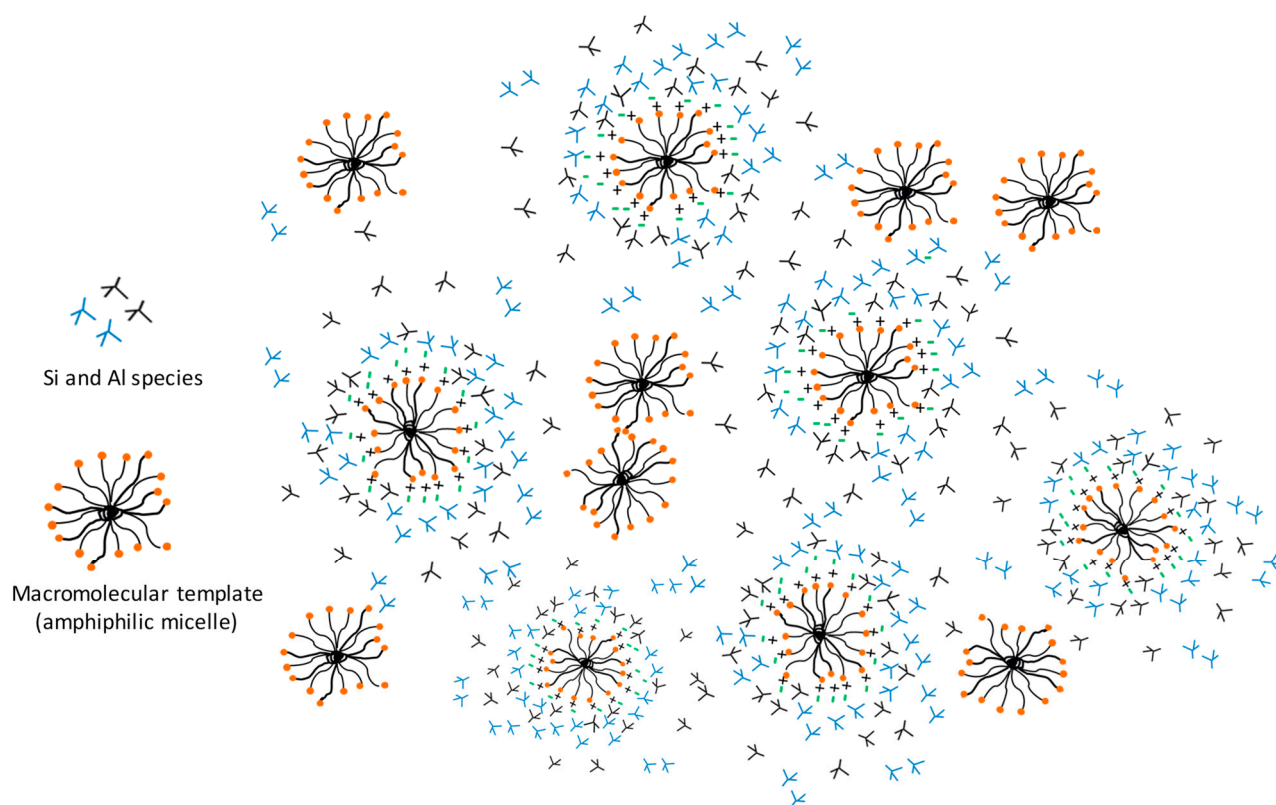


**Figure 7.** The schematic representation of macromolecular surfactant encapsulated gradually by Si and Al species to form mesopores in the final zeolite structure.

### 7. Influence of SDAs on the Size of Zeolite Particles: Giant (Several Microns/Millimeter Scale) Crystals versus Miniaturized (Nanoscale) Zeolites Particles

The main key factor for the synthesis of large crystals of zeolites is the addition of an agent that can control the nucleation rate and keep it low. Fluoride is the most famous mineralizer, which can produce large zeolitic crystals by suppressing the nucleation step and favoring the growth step under low supersaturation conditions. Interestingly, organic SDAs affect both the morphology and size of the zeolite crystal. For instance, the MFI-type zeolite synthesized using conventional  $\text{TPA}^+$ , differs in morphology and size (i.e., coffin-shaped crystals, 5  $\mu\text{m}$  in magnitude) compared to those prepared using diquatery ammonium cations, which give various morphologies such as octagonal, leaf-shaped and platelike crystals. The crystal size increases up to 5  $\mu\text{m}$  only in the case of  $(\text{C}_3\text{H}_7)_3\text{N}^+(\text{CH}_2)_6\text{N}^+(\text{C}_3\text{H}_7)_3$ , while other amines reduce the crystal size to 1  $\mu\text{m}$  [129]. Larger crystals of the MFI-type zeolite were synthesized using tetra-, tri- or dipropylammonium fluoride molecules [130]. In addition, the morphology of TPA-MFI showed to be more elongated, and while using other SDAs, cubic-like morphologies were obtained [131]. In another study, using pyrrolidine as the SDA, several zeolites such as ZSM-5, ZSM-35, ZSM-39, ZSM-48 and KZ-1 were prepared and it was reported that both morphology and size of ZSM-5 prepared by pyrrolidine differentiate from TPA-ZSM-5 [132]. The effect of SDA quantity on the morphology and size of zeolite crystals has also been studied for TPA-MFI and proved that lower amounts of SDA increase the size of crystals with a rod-like morphology [133,134]. Application of  $\text{TEA}^+$  in the synthesis of zeolite Y has shown to be effective for the synthesis of zeolite Y with large crystal sizes between 210–245  $\mu\text{m}$  [135].

In contrast, the application of large amounts of SDAs leads to the synthesis of zeolite crystals in the nano-range [136,137]. Traditionally, reducing the zeolite particle size to the nano-scale requires a high nucleation rate, and meanwhile, the alkali metal concentration should be decreased to prevent particle aggregation. For compensating for the lack of alkali metals, large quantities of SDAs (e.g., alkyl amines) should be used, which in turn,

decrease the size of zeolite particles. A series of zeolites that can be synthesized in the nano dimension using SDAs are shown in Table 2. Similar to the mono-templating, the co-templating technique also demonstrates similar effects on zeolite particle size. For example, the crystal size of SAPO-34 synthesized using three templates (i.e., TEA<sup>+</sup>, trimethylamine and morpholine) was reduced from 3.25 μm to 0.64 μm at certain molar ratios between the above-mentioned SDAs [116]. In line with this, by increasing the size and charge of SDA, the zeolite crystal size is decreased as also reported for CHA type zeolites [114].

**Table 2.** Effects of organic SDAs on the particle size of zeolites [69].

Entry	Zeolite Topology	Zeolite Name	SDA
1	EDI	Linde F	-
2	EDI	Nanosized Linde F	TEA <sup>+</sup>
3	FAU	Linde Type Y	-
4	FAU	Nanosized Linde Type Y	TMA <sup>+</sup>
5	LTA	Linde Type A	-
6	LTA	Nanosized Linde Type A	TMA <sup>+</sup>

## 8. Summary and Concluding Remarks

This mini-review has represented the effect of SDAs on zeolite physicochemical properties. Although in recent decades, several new SDAs have been invented, defining optimum properties for an SDA molecule is not straightforward. To look more closely at SDA development, one can see that several parameters interplay in this process, namely the interaction between SDA and zeolite precursors or with solvents, structural stability (rigidity), degrees of hydrophobicity, and so forth. The impacts of quantity and nature of SDA are also important in the zeolite synthesis procedure and should be taken into account. Developing an in-depth knowledge about these features is still in progress and requires comprehensive insight into their multi-task role in zeolite crystallization. Altogether, having all these complexities, the combination of computational and experimental approaches is essential for the assessment of available SDAs, as well as modelling of new species to outline protocols for the synthesis of new alternative SDAs.

**Author Contributions:** Z.A.P.: writing, the review design, reference collection and preparation of original draft, K.O.S.: review, editing, directing and general guidance, All authors have read and agreed to the published version of the manuscript.

**Funding:** This research is a review and received no external funding.

**Data Availability Statement:** Not applicable.

**Conflicts of Interest:** The authors declare no conflict of interest.

## References

- Rhodes, C.J. Properties and applications of zeolites. *Sci. Prog.* **2010**, *93*, 223–284. [[CrossRef](#)] [[PubMed](#)]
- Rimer, J.D. Rational design of zeolite catalysts. *Nat. Catal.* **2018**, *1*, 488–489. [[CrossRef](#)]
- Weitkamp, J. Zeolites and catalysis. *Solid State Ion.* **2000**, *131*, 175–188. [[CrossRef](#)]
- Ackley, M.W.; Rege, S.U.; Saxena, H. Application of natural zeolites in the purification and separation of gases. *Microporous Mesoporous Mater.* **2003**, *61*, 25–42. [[CrossRef](#)]
- Feng, C.; Jiaqiang, E.; Han, W.; Deng, Y.; Zhang, B.; Zhao, X. Key technology and application analysis of zeolite adsorption for energy storage and heat-mass transfer process: A review. *Renew. Sustain. Energy Rev.* **2021**, *144*, 110954–110980. [[CrossRef](#)]
- Thompson, R.W. Recent Advances in the Understanding of Zeolite Synthesis. *Mol. Sieves* **1998**, *1*, 1–33. [[CrossRef](#)]
- Barrer, R.M. Zeolites and their synthesis. *Zeolites* **1981**, *1*, 130–140. [[CrossRef](#)]
- Barrer, R.M. Syntheses and reactions of mordenite. *J. Chem. Soc.* **1948**, 435, 2158–2163. [[CrossRef](#)]
- Yu, J. Chapter 3 Synthesis of zeolites Introd. *Zeolite Sci. Practice* **2007**, *168*, 39–103.
- Reed, T.B.; Breck, D.W. Crystalline Zeolites. II. Crystal Structure of Synthetic Zeolite, Type A. *J. Am. Chem. Soc.* **1956**, *545*, 5972–5977. [[CrossRef](#)]
- Breck, D.W. Crystalline Zeolite Y. U.S. Patent 3,130,007, 21 April 1964.

12. Argauer, R.J.; Landolt, G.R. Crystalline Zeolite ZSM-5 and Method of Preparing the Same. U.S. Patent 3,702,886, 14 November 1972.
13. Wadlinger, R.L.; Kerr, G.T.; Rosinski, E.J. Catalytic Composition of a Crystalline Zeolite. U.S. Patent 3,308,069, 7 March 1967.
14. Karami, D.; Mahinpey, N. The synthesis of novel zeolite Y nanoparticles using mesoporous silica with a temperature controlling method. *Can. J. Chem. Eng.* **2014**, *92*, 671–675. [[CrossRef](#)]
15. Rollmann, L.D.; Schlenker, J.L.; Lawton, S.L.; Kennedy, C.L.; Kennedy, G.J.; Doren, D.J. On the Role of Small Amines in Zeolite Synthesis. *J. Phys. Chem. B* **1999**, *34*, 7175–7183. [[CrossRef](#)]
16. Burton, A. Recent trends in the synthesis of high-silica zeolites. *Catal. Rev.* **2018**, *60*, 132–175. [[CrossRef](#)]
17. Li, J.; Corma, A.; Yu, J. Synthesis of new zeolite structures. *Chem. Soc. Rev.* **2015**, *44*, 7112–7127. [[CrossRef](#)]
18. Li, Y.; Cao, H.; Yu, J. Toward a New Era of Designed Synthesis of Nanoporous Zeolitic Materials. *ACS Nano* **2018**, *12*, 4096–4104. [[CrossRef](#)]
19. Davis, M.E.; Lobo, R.F. Zeolite and Molecular Sieve Synthesis. *Chem. Mater.* **1992**, *4*, 756–768. [[CrossRef](#)]
20. Wang, Z.; Yu, J.; Xu, R. Needs and trends in rational synthesis of zeolitic materials. *Chem. Soc. Rev.* **2012**, *41*, 1729–1741. [[CrossRef](#)]
21. Li, S.; Li, J.; Dong, M.; Fan, S.; Zhao, T. Strategies to control zeolite particle morphology. *Chem. Soc. Rev.* **2019**, *48*, 885–907. [[CrossRef](#)]
22. Schüth, F. Engineering porous catalytic materials. *Annu. Rev. Mater. Res.* **2005**, *35*, 209–238. [[CrossRef](#)]
23. Lee, H.; Zones, S.I.; Davis, M.E. Zeolite synthesis using degradable structure-directing agents and pore-filling agents. *J. Phys. Chem. B* **2005**, *109*, 2187–2191. [[CrossRef](#)]
24. Sakai, M.; Hori, H.; Matsukata, M. Alkaline-treatment with pore-filling agent for defect-healing of zeolite membrane. *Microporous Mesoporous Mater.* **2022**, *336*, 111901–111906. [[CrossRef](#)]
25. Cambor, M.A.; Corma, A.; Díaz-Cabañas, M.J.; Baerlocher, C. Synthesis and structural characterization of MWW type zeolite ITQ-1, the pure silica analog of MCM-22 and SSZ-25. *J. Phys. Chem. B* **1998**, *102*, 44–511. [[CrossRef](#)]
26. Ouyang, X.; Hwang, S.J.; Runnebaum, R.C.; Xie, D.; Wanglee, Y.J.; Rea, T.; Zones, S.I.; Katz, A. Single-step delamination of a MWW borosilicate layered zeolite precursor under mild conditions without surfactant and sonication. *J. Am. Chem. Soc.* **2014**, *136*, 1449–1461. [[CrossRef](#)]
27. Pinar, A.B.; Wright, P.A.; Gómez-Hortigüela, L.; Pérez-Pariente, J. Synthesis of ferrierite zeolite with pyrrolidine as structure directing agent: A combined X-ray diffraction and computational study. *Microporous Mesoporous Mater.* **2010**, *129*, 164–172. [[CrossRef](#)]
28. Zones, S.I.; Burton, A.W. Diquaternary structure-directing agents built upon charged imidazolium ring centers and their use in synthesis of one-dimensional pore zeolites. *J. Mater. Chem.* **2005**, *15*, 4215–4223. [[CrossRef](#)]
29. Beck, L.W.; E Davis, M. Alkylammonium polycations as structure-directing agents in MFI zeolite synthesis. *Microporous Mesoporous Mater.* **1998**, *22*, 107–114. [[CrossRef](#)]
30. Gómez-Hortigüela, L.; Márquez-Álvarez, C.; Grande-Casas, M.; García, R.; Pérez-Pariente, J. Tailoring the acid strength of microporous silicoaluminophosphates through the use of mixtures of templates: Control of the silicon incorporation mechanism. *Microporous Mesoporous Mater.* **2009**, *121*, 129–137. [[CrossRef](#)]
31. Liu, P.; Ren, J.; Sun, Y. Influence of template on Si distribution of SAPO-11 and their performance for n-paraffin isomerization. *Microporous Mesoporous Mater.* **2008**, *114*, 365–372. [[CrossRef](#)]
32. Lewis, D.W.; Freeman, C.M.; Catlow, C.R.A. Predicting the templating ability of organic additives for the synthesis of microporous materials. *J. Phys. Chem.* **1995**, *99*, 11194–11202. [[CrossRef](#)]
33. Yang, X.; Cambor, M.A.; Lee, Y.; Liu, H.; Olson, D.H. Synthesis and crystal structure of as-synthesized and calcined pure silica zeolite ITQ-12. *J. Am. Chem. Soc.* **2004**, *126*, 10403–10409. [[CrossRef](#)]
34. Millini, R. Application of modeling in zeolite science. *Catal. Today* **1998**, *41*, 41–51. [[CrossRef](#)]
35. Araya, A.; Lowe, B.M. Effect of organic species on the synthesis and properties of ZSM-5. *Zeolites* **1986**, *6*, 111–118. [[CrossRef](#)]
36. Corma, A.; Navarro, M.T.; Rey, F.; Rius, J.; Valencia, S. Pure polymorph C of zeolite beta synthesized by using framework isomorphous substitution as a structure-directing mechanism. *Angew. Chem.* **2001**, *113*, 2337–2340. [[CrossRef](#)]
37. Feast, S.; Rafiq, M.; Siddiqui, H.; Wells, R.P.; Willock, D.J.; King, F.; Rochester, C.H.; Bethell, D.; Bulman Page, f.c.; Hutchings, G.J. Enantioselective dehydration of butan-2-ol using zeolite Y modified with dithiane oxides. *J. Catal.* **1997**, *167*, 533–542. [[CrossRef](#)]
38. Mizukami, F. Application of zeolite membranes, films and coatings. *Stud. Surf. Sci. Catal.* **1999**, *125*, 1–12. [[CrossRef](#)]
39. Sastre, G.; Leiva, S.; Sabater, M.J.; Gimenez, I.; Rey, F.; Valencia, S.; Corma, A. Computational and Experimental Approach to the Role of Structure-Directing Agents in the Synthesis of Zeolites: The Case of Cyclohexyl Alkyl Pyrrolidinium Salts in the Synthesis of Zeolites. *J. Phys. Chem.* **2003**, *107*, 5432–5440. [[CrossRef](#)]
40. Corma, A.; Díaz-Cabañas, M.J.; Rey, F.; Nicolopoulos, S.; Boulahya, K. ITQ-15: The first ultralarge pore zeolite with a bi-directional pore system formed by intersecting 14- and 12-ring channels, and its catalytic implications. *Chem. Commun.* **2004**, *4*, 1356–1357. [[CrossRef](#)]
41. Corma, A.; Díaz-Cabañas, M.J.; Martínez-Triguero, J.; Rey, F.; Rius, J. A large-cavity zeolite with wide pore windows and potential as an oil refining catalyst. *Lett. Nat.* **2002**, *418*, 1277–1280. [[CrossRef](#)]
42. Feliczak-guzik, A. Microporous and Mesoporous Materials, Hierarchical zeolites: Synthesis and catalytic properties. *Microporous Mesoporous Mater.* **2018**, *259*, 33–45. [[CrossRef](#)]

43. Turta, N.A.; De Luca, P.; Bilba, N.; Nagy, J.B.; Nastro, A. Synthesis of titanosilicate ETS-10 in presence of cetyltri-methylammonium bromide. *Microporous Mesoporous Mater.* **2008**, *112*, 425–431. [[CrossRef](#)]
44. Pavel, C.C.; Nagy, J.B.; Bilba, N.; Nastro, A.; Perri, C.; Vuono, D.; De Luka, P.; Asaftei, I.V. Influence of the TAABr salts on the crystallization of ETS-10. *Microporous Mesoporous Mater.* **2004**, *71*, 77–85. [[CrossRef](#)]
45. Perez-Ramirez, J.; Christensen, C.H.; Egeblad, K.; Christensen, C.H.; Groen, J.C. Hierarchical zeolites: Enhanced utilisation of microporous crystals in catalysis by advances in materials design. *Chem. Soc. Rev.* **2008**, *37*, 2530–2542. [[CrossRef](#)] [[PubMed](#)]
46. Martínez, J.G.; Garcia, J. Realizing the Commercial Potential of Hierarchical Zeolites—Final Realizing the Commercial Potential of Hierarchical Zeolites: New Opportunities in Catalytic Cracking. *ChemCatChem* **2014**, *6*, 46–66. [[CrossRef](#)]
47. Asgar Pour, Z.; Boer, D.G.; Fang, S.; Tang, Z.; Pescarmona, P.P. Bimetallic Zeolite Beta Beads with Hierarchical Porosity as Brønsted-Lewis Solid Acid Catalysts for the Synthesis of Methyl Lactate. *Catalysts* **2021**, *11*, 1346. [[CrossRef](#)]
48. Garcia-Martinez, J.; Cazorla-Amorós, D.; Linares-Solano, A.; Lin, J. Synthesis and characterisation of MFI-type zeolites supported on carbon materials. *Microporous Mesoporous Mater.* **2001**, *42*, 255–268. [[CrossRef](#)]
49. Tao, Y.; Kanoh, H.; Kaneko, K. ZSM-5 Monolith of Uniform Mesoporous Channels. *J. Am. Chem. Soc.* **2003**, *125*, 6044–6045. [[CrossRef](#)]
50. Lee, Y.J.; Lee, J.S.; Park, Y.S.; Yoon, K.B. Synthesis of Large Monolithic Zeolite Foams with Variable Macropore Architectures. *Adv. Mater.* **2001**, *13*, 1259–1263. [[CrossRef](#)]
51. Wiśniewska, M.; Fijałkowska, G.; Nosal-Wiercińska, A.; Franus, M.; Panek, R. Adsorption mechanism of poly(vinyl alcohol) on the surfaces of synthetic zeolites: Sodalite, Na-P1 and Na-A. *Adsorption* **2019**, *25*, 567–574. [[CrossRef](#)]
52. Panek, R.; Medykowska, M.; Szewczuk-Karpisz, K.; Wiśniewska, M. Comparison of Physicochemical Properties of Fly Ash Precursor, Na-P1(C) Zeolite–Carbon Composite and Na-P1 Zeolite—Adsorption Affinity to Divalent Pb and Zn Cations. *Materials* **2021**, *14*, 3018. [[CrossRef](#)]
53. Panek, R.; Medykowska, M.; Wiśniewska, M.; Szewczuk-Karpisz, K.; Jędruchniewicz, K.; Franus, M. Simultaneous Removal of Pb<sup>2+</sup> and Zn<sup>2+</sup> Heavy Metals Using Fly Ash Na-X Zeolite and Its Carbon Na-X(C) Composite. *Materials* **2021**, *14*, 2832. [[CrossRef](#)]
54. Sebakhy, K.O.; Vitale, G.; Pereira-Almao, P.R. Production of Highly Dispersed Ni within Nickel Silicate Materials with the MFI Structure for the Selective Hydrogenation of Olefins. *Ind. Eng. Chem. Res.* **2019**, *58*, 8597–8611. [[CrossRef](#)]
55. Barrer, R.M.; Denny, P.J. Hydrothermal Chemistry of the silicates. Part IX. Nitrogenous Aluminosilicates. *J. Chem. Soc.* **1961**, 971–982. [[CrossRef](#)]
56. Kerr, G.T. Chemistry of Crystalline Aluminosilicates. II. The Synthesis and Properties of Zeolite ZK-4. *Inorg. Chem.* **1966**, *5*, 1537–1539. [[CrossRef](#)]
57. Goepper, M.; Li, H.-X.; Davis, M.E. A possible role of alkali metal ions in the synthesis of pure-silica molecular sieves. *J. Chem. Soc. Chem. Commun.* **1992**, *22*, 1665–1666. [[CrossRef](#)]
58. Lobo, R.F.; Zones, S.I.; Davis, M.E. Structure-direction in zeolite synthesis. *J. Incl. Phenom. Mol. Recognit. Chem.* **1995**, *21*, 47–78. [[CrossRef](#)]
59. Martínez, C.; Corma, A. Inorganic molecular sieves: Preparation, modification and industrial application in catalytic processes. *Coord. Chem. Rev.* **2011**, *255*, 1558–1580. [[CrossRef](#)]
60. Corma, A.; Rey, F.; Rius, J.; Sabater, M.J.; Valencia, S. Supramolecular self-assembled molecules as organic directing agent for synthesis of zeolites. *Nature* **2004**, *431*, 287–290. [[CrossRef](#)]
61. Xie, B.; Zhang, H.; Yang, C.; Liu, S.; Ren, L.; Zhang, L.; Meng, X.; Yilmaz, B.; Müller, U.; Xiao, F.-S. Seed-directed synthesis of zeolites with enhanced performance in the absence of organic templates. *Chem. Commun.* **2011**, *47*, 3945–3947. [[CrossRef](#)]
62. Moliner, M.; Rey, F.; Corma, A. Towards the Rational Design of Efficient Organic Structure-Directing Agents for Zeolite Synthesis. *Angew. Chem. Int. Ed.* **2013**, *52*, 13880–13889. [[CrossRef](#)]
63. Yabushita, M.; Osuga, R.; Muramatsu, A. Control of location and distribution of heteroatoms substituted isomorphously in framework of zeolites and zeotype materials. *CrystEngComm* **2021**, *23*, 6226–6233. [[CrossRef](#)]
64. Burton, A.W.; Zones, S.I.; Elomari, S. The chemistry of phase selectivity in the synthesis of high-silica zeolites. *Curr. Opin. Colloid Interface Sci.* **2005**, *10*, 211–219. [[CrossRef](#)]
65. Corminboeuf, C.; Tran, F.; Weber, J. The role of density functional theory in chemistry: Some historical landmarks and applications to zeolites. *J. Mol. Struct. Theochem* **2006**, *762*, 1–7. [[CrossRef](#)]
66. Ma, S.; Liu, Z.P. The Role of Zeolite Framework in Zeolite Stability and Catalysis from Recent Atomic Simulation. *Top. Catal.* **2022**, *65*, 59–68. [[CrossRef](#)]
67. Di Iorio, J.R.; Li, S.; Jones, C.B.; Nimlos, C.T.; Wang, Y.; Kunkes, E.; Vattipalli, V.; Prasad, S.; Moini, A.; Schneider, W.F.; et al. Cooperative and Competitive Occlusion of Organic and Inorganic Structure-Directing Agents within Chabazite Zeolites Influences Their Aluminum Arrangement. *J. Am. Chem. Soc.* **2020**, *142*, 4807–4819. [[CrossRef](#)]
68. Nimlos, C.T.; Hoffman, A.J.; Hur, Y.G.; Lee, B.J.; Di Iorio, J.R.; Hibbitts, D.D.; Gounder, R. Experimental and Theoretical Assessments of Aluminum Proximity in MFI Zeolites and Its Alteration by Organic and Inorganic Structure-Directing Agents. *Chem. Mater.* **2020**, *32*, 9277–9298. [[CrossRef](#)]
69. Baerlocher, C.; McCusker, L.B.; Olson, D.H. *Atlas of Zeolite Framework Types*; Elsevier: Amsterdam, The Netherlands, 2007.
70. Robson, H.; Lillerud, K.P. (Eds.) *Verified Synthesis of Zeolitic Materials*; Elsevier: Amsterdam, The Netherlands, 2001.
71. Goretsky, A.V.; Beck, L.W.; I Zones, S.; E Davis, M. Influence of the hydrophobic character of structure-directing agents for the synthesis of pure-silica zeolites. *Microporous Mesoporous Mater.* **1999**, *28*, 387–393. [[CrossRef](#)]

72. Gies, H.; Marker, B. The structure-controlling role of organic templates for the synthesis of porosils in the systems SiO<sub>2</sub>/template/H<sub>2</sub>O. *Zeolites* **1992**, *12*, 42–49. [CrossRef]
73. Gómez-Hortigüela, L.; Corà, F.; Catlow, C.R.A.; Pérez-Pariente, J. Computational Study of the Structure-Directing Effect of Benzylpyrrolidine and Its Fluorinated Derivatives in the Synthesis of the Aluminophosphate AlPO-5. *J. Am. Chem. Soc.* **2004**, *126*, 12097–12102. [CrossRef]
74. Davis, M.E. Zeolites from a Materials Chemistry Perspective. *Chem. Mater.* **2013**, *26*, 239–245. [CrossRef]
75. Sastre, G.; Pulido, A.; Castañeda, R.; Corma, A. Effect of the Germanium Incorporation in the Synthesis of EU-1, ITQ-13, ITQ-22, and ITQ-24 Zeolites. *J. Phys. Chem. B* **2004**, *108*, 8830–8835. [CrossRef]
76. Leon, S.; Sastre, G. Zeolite Phase Selectivity Using the Same Organic Structure-Directing Agent in Fluoride and Hydroxide Media. *J. Phys. Chem. C* **2022**, *126*, 2078–2087. [CrossRef]
77. Strohmaier, K.G.; Vaughan, D.E.W. Structure of the First Silicate Molecular Sieve with 18-Ring Pore Openings, ECR-34. *J. Am. Chem. Soc.* **2003**, *125*, 16035–16039. [CrossRef] [PubMed]
78. Baerlocher, C.; McCusker, L.B. Database of Zeolite Structures. Available online: <http://www.iza-structure.org/databases/> (accessed on 17 March 2022).
79. Kubota, Y.; Helmkamp, M.M.; Zones, S.I.; Davis, M.E. Properties of organic cations that lead to the structure-direction of high-silica molecular sieves. *Microporous Mater.* **1996**, *6*, 213–229. [CrossRef]
80. Liebau, F. Zeolites and clathrasils—Two distinct classes of framework silicates. *Zeolites* **1983**, *3*, 191–193. [CrossRef]
81. Casci, J.L.; Barrie, M.; Whittam, T.V. Zeolite EU-1 and a Method of Making Zeolite EU-1. U.S. Patent 4,537,754, 11 June 1981.
82. Schlenker, J.; Rohrbaugh, W.; Chu, P.; Valyocsik, E.; Kokotailo, G. The framework topology of ZSM-48: A high silica zeolite. *Zeolites* **1985**, *5*, 355–358. [CrossRef]
83. Nakagawa, Y.; Lee, G.; Harris, T.; Yuen, L.; Zones, S. Guest/host relationships in zeolite synthesis: Ring-substituted piperidines and the remarkable adamantane mimicry by 1-azonio spiro [5.5] undecanes. *Microporous Mesoporous Mater.* **1998**, *22*, 69–85. [CrossRef]
84. Baerlocher, C.; Gramm, F.; Massüger, L.; McCusker, L.B.; He, Z.; Hovmöller, S.; Zou, X. Structure of the Polycrystalline Zeolite Catalyst IM-5 Solved by Enhanced Charge Flipping. *Science* **2007**, *315*, 1113–1116. [CrossRef]
85. Jackowski, A.; Zones, S.; Burton, A. A study on zeolite synthesis from diquaternary ammonium compounds; the effect of changing end-group heterocycles in the HF/SiO<sub>2</sub> synthesis of molecular sieves. *Stud. Surf. Sci. Catal.* **2008**, *174*, 111–116. [CrossRef]
86. Gramm, F.; Baerlocher, C.; McCusker, L.B.; Warrender, S.J.; Wright, P.A.; Han, B.; Hong, S.B.; Liu, Z.; Ohsuna, T.; Terasaki, O. Complex zeolite structure solved by combining powder diffraction and electron microscopy. *Nature* **2006**, *444*, 79–81. [CrossRef]
87. Jackowski, A.; Zones, S.I.; Hwang, S.-J.; Burton, A.W. Diquaternary Ammonium Compounds in Zeolite Synthesis: Cyclic and Polycyclic N-Heterocycles Connected by Methylene Chains. *J. Am. Chem. Soc.* **2009**, *131*, 1092–1100. [CrossRef]
88. Zones, S. Synthesis of pentasil zeolites from sodium silicate solutions in the presence of quaternary imidazole compounds. *Zeolites* **1989**, *9*, 458–467. [CrossRef]
89. Barrett, P.A.; Boix, T.; Puche, M.; Olson, D.H.; Jordan, E.; Koller, H.; Cambor, M.A. ITQ-12: A new microporous silica polymorph potentially useful for light hydrocarbon separations. *Chem. Commun.* **2003**, *17*, 2114–2115. [CrossRef] [PubMed]
90. Zones, S.I.; Burton, A.W. Molecular Sieve SSZ-70 Composition of Matter and Synthesis Thereof. U.S. Patent 7,108,842 B2, 19 September 2006.
91. Lorgouilloux, Y.; Dodin, M.; Paillaud, J.-L.; Caullet, P.; Michelin, L.; Josien, L.; Ersen, O.; Bats, N. IM-16: A new microporous germanosilicate with a novel framework topology containing d4r and mtw composite building units. *J. Solid State Chem.* **2009**, *182*, 622–629. [CrossRef]
92. Parnham, E.R.; Morris, R.E. The Ionothermal Synthesis of Cobalt Aluminophosphate Zeolite Frameworks. *J. Am. Chem. Soc.* **2006**, *128*, 2204–2205. [CrossRef] [PubMed]
93. Zones, S.I.; Nakagawa, Y.; Yuen, A.L.T.; Harris, T.V. Guest/Host Interactions in High Silica Zeolite Synthesis: [5.2.1.0<sup>2.6</sup>]Tricyclodecanes as Template Molecule. *J. Am. Chem. Soc.* **1996**, *118*, 7558–7567. [CrossRef]
94. Calabro, D.C.; Cheng, J.C.; Crane, R.A.; Kresge, C.T.; Dhingra, S.S.; Steckel, M.A.; Stern, D.L.; Weston, S.C. Synthetic Porous Crystalline MCM-68, Its Synthesis and Use. U.S. Patent 6,049,018, 11 April 2000.
95. Dorset, D.L.; Weston, S.C.; Dhingra, S.S. Crystal Structure of Zeolite MCM-68: A New Three-Dimensional Framework with Large Pores. *J. Phys. Chem. B* **2006**, *110*, 2045–2050. [CrossRef]
96. Lee, G.S.; Zones, S.I. Polymethylated [4.1.1] Octanes Leading to Zeolite SSZ-50. *J. Solid State Chem.* **2002**, *167*, 289–298. [CrossRef]
97. Elomari, S.; Burton, A.; Medrud, R.C.; Grosse-Kunstleve, R. The synthesis, characterization, and structure solution of SSZ-56: An extreme example of isomer specificity in the structure direction of zeolites. *Microporous Mesoporous Mater.* **2009**, *118*, 325–333. [CrossRef]
98. Elomari, S. Process for Preparing Zeolites Using Pyrrolidinium Cations. U.S. Patent 6,616,911 b2, 9 September 2003.
99. Burton, A.; Elomari, S.; Medrud, R.C.; Chan, I.Y.; Chen, C.-Y.; Bull, L.M.; Vittoratos, E.S. The Synthesis, Characterization, and Structure Solution of SSZ-58: A Novel Two-Dimensional 10-Ring Pore Zeolite with Previously Unseen Double 5-Ring Subunits. *J. Am. Chem. Soc.* **2003**, *125*, 1633–1642. [CrossRef]
100. Burton, A.; Elomari, S.; Chen, C.-Y.; Medrud, R.C.; Chan, I.Y.; Bull, L.M.; Kibby, C.; Harris, T.V.; Zones, S.I.; Vittoratos, E.S. SSZ-53 and SSZ-59: Two Novel Extra-Large Pore Zeolites. *Chem. A Eur. J.* **2003**, *9*, 5737–5748. [CrossRef]

101. Elomari, S.; Burton, A.W.; Ong, K.; Pradhan, A.R.; Chan, I.Y. Synthesis and Structure Solution of Zeolite SSZ-65. *Chem. Mater.* **2007**, *19*, 5485–5492. [[CrossRef](#)]
102. Jiang, J.; Yu, J.; Corma, A. Extra-Large-Pore Zeolites: Bridging the Gap between Micro and Mesoporous Structures. *Angew. Chem. Int. Ed.* **2010**, *49*, 3120–3145. [[CrossRef](#)] [[PubMed](#)]
103. Delprato, F.; Delmotte, L.; Guth, J.; Huve, L. Synthesis of new silica-rich cubic and hexagonal faujasites using crown-etherbased supramolecules as templates. *Zeolites* **1990**, *10*, 546–552. [[CrossRef](#)]
104. Pinar, A.B.; Marquez-Alvarez, C.; Grande-Casas, M.; Pérez-Pariente, J. Template-controlled acidity and catalytic activity of ferrierite crystals. *J. Catal.* **2009**, *263*, 258–265. [[CrossRef](#)]
105. Marquez-Alvarez, C.; Pinar, A.B.; Garcia, R.; Grande-Casas, M.; Pérez-Pariente, J. Influence of Al Distribution and Defects Concentration of Ferrierite Catalysts Synthesized From Na-Free Gels in the Skeletal Isomerization of n-Butene. *Top. Catal.* **2009**, *52*, 1281–1291. [[CrossRef](#)]
106. Fernandes, A.; Ribeiro, F.; Lourenço, J.; Gabelica, Z. An elegant way to increase acidity in SAPOs: Use of methylamine as co-template during synthesis. *Stud. Surf. Sci. Catal.* **2008**, *174*, 281–284. [[CrossRef](#)]
107. Li, L.; Zhang, F. Effect of templates on synthesis of SAPO-41 and their catalytic performance in n-octane hydroisomerization. *Stud. Surf. Sci. Catal.* **2007**, *170*, 397–402.
108. Chatelain, T.; Patarin, J.; Souldard, M.; Guth, J.; Schulz, P. Synthesis and characterization of high-silica EMT and FAU zeolites prepared in the presence of crown-ethers with either ethylene glycol or 1,3,5-trioxane. *Zeolites* **1995**, *15*, 90–96. [[CrossRef](#)]
109. Pelrine, B.P. Synthesis of ZSM-39. U.S. Patent 4,259,306, 31 March 1981.
110. Jacobs, P.A.; Martens, J.A. *Synthesis of High-Silica Aluminosilicate Zeolites*; Elsevier: Amsterdam, The Netherlands, 1987.
111. Schlenker, J.L.; Dwyer, F.G.; Jenkins, E.E.; Rohrbaugh, W.J.; Kokotailo, G.T.; Meier, W.M. Crystal structure of a synthetic high silica zeolite—ZSM-39. *Nature* **1981**, *294*, 340–342. [[CrossRef](#)]
112. de Saldarriaga, L.S.; Saldarriaga, C.; Davis, M.E. Investigations into the nature of a silicoaluminophosphate with the faujasite structure. *J. Am. Chem. Soc.* **1987**, *109*, 2686–2691. [[CrossRef](#)]
113. Franco, M.; Pérez-Pariente, J.; Misud, A.; Blasco, T.; Sanz, J. Crystallization kinetics of SAPO-37. *Zeolites* **1992**, *12*, 386–394. [[CrossRef](#)]
114. Carreon, M.A.; Li, S.; Falconer, J.L.; Noble, R.D. SAPO-34 Seeds and Membranes Prepared Using Multiple Structure Directing Agents. *Adv. Mater.* **2008**, *20*, 729–732. [[CrossRef](#)]
115. Xu, J.; Haw, K.-G.; Li, Z.; Pati, S.; Wang, Z.; Kawi, S. A mini-review on recent developments in SAPO-34 zeolite membranes and membrane reactors. *React. Chem. Eng.* **2020**, *6*, 52–66. [[CrossRef](#)]
116. Masoumi, S.; Towfighi, J.; Mohamadizadeh, A.; Kooshki, Z.; Rahimi, K. Tri-templates synthesis of SAPO-34 and its performance in MTO reaction by statistical design of experiments. *Appl. Catal. A Gen.* **2015**, *493*, 103–111. [[CrossRef](#)]
117. Zones, S.I.; Hwang, S.-J.; Davis, M.E. Studies of the Synthesis of SSZ-25 Zeolite in a “Mixed-Template” System. *Chem. Eur. J.* **2001**, *7*, 1990–2001. [[CrossRef](#)]
118. Zones, S.I.; Hwang, S.-J. Synthesis of High Silica Zeolites Using a Mixed Quaternary Ammonium Cation, Amine Approach: Discovery of Zeolite SSZ-47. *Chem. Mater.* **2001**, *14*, 313–320. [[CrossRef](#)]
119. Blackwell, C.S.; Broach, R.W.; Gatter, M.G.; Holmgren, J.S.; Jan, D.-Y.; Lewis, G.J.; Mezza, B.J.; Mezza, T.M.; Miller, M.A.; Moscoso, J.G.; et al. Open-Framework Materials Synthesized in the TMA/TEA Mixed-Template System: The New Low Si/Al Ratio Zeolites UZM-4 and UZM-5. *Angew. Chem. Int. Ed.* **2003**, *42*, 1737–1740. [[CrossRef](#)]
120. Zones, S.I.; Nakagawa, Y. Preparation of Zeolites Using Organic Template and Amine. U.S. Patent 5,785,947, 28 July 1998.
121. Kalantari, N.; Farzi, A.; Delibaş, N.; Niaei, A.; Salari, D. Synthesis of multiple-template zeolites with various compositions and investigation of their catalytic properties. *Res. Chem. Intermed.* **2021**, *47*, 4957–4984. [[CrossRef](#)]
122. Ma, H.; Lin, H.; Liu, X.; Lü, H.; Zhu, Z. In situ structural reconstruction triggers the hydrothermal synthesis of hierarchical Ti-Beta zeolites for oxidative desulfurization. *Mater. Chem. Front.* **2021**, *5*, 6101–6113. [[CrossRef](#)]
123. Jia, X.; Khan, W.; Wu, Z.; Choi, J.; Yip, A.C. Modern synthesis strategies for hierarchical zeolites: Bottom-up versus top-down strategies. *Adv. Powder Technol.* **2018**, *30*, 467–484. [[CrossRef](#)]
124. Wang, C.; Yang, M.; Tian, P.; Xu, S.; Yang, Y.; Wang, D.; Yuan, Y.; Liu, Z. Dual template-directed synthesis of SAPO-34 nanosheet assemblies with improved stability in the methanol to olefins reaction. *J. Mater. Chem. A* **2015**, *3*, 5608–5616. [[CrossRef](#)]
125. Xu, H.; Wu, P. Two-dimensional zeolites in catalysis: Current state-of-the-art and perspectives. *Catal. Rev.* **2021**, *63*, 234–301. [[CrossRef](#)]
126. Huang, L.; Guo, W.; Deng, P.; Xue, Z.; Li, Q. Investigation of Synthesizing MCM-41/ZSM-5 Composites. *J. Phys. Chem. B* **2000**, *104*, 2817–2823. [[CrossRef](#)]
127. Na, K.; Choi, M.; Ryoo, R. Recent advances in the synthesis of hierarchically nanoporous zeolites. *Microporous Mesoporous Mater.* **2013**, *166*, 3–19. [[CrossRef](#)]
128. Na, K.; Jo, C.; Kim, J.; Cho, K.; Jung, J.; Seo, Y.; Messinger, R.J.; Chmelka, B.F.; Ryoo, R. Directing Zeolite Structures into Hierarchically Nanoporous Architectures. *Science* **2011**, *333*, 328–332. [[CrossRef](#)]
129. Bonilla, G.; Díaz, I.; Tsapatsis, M.; Jeong, H.-K.; Lee, A.Y.; Vlachos, D.G. Zeolite (MFI) Crystal Morphology Control Using Organic Structure-Directing Agents. *Chem. Mater.* **2004**, *16*, 5697–5705. [[CrossRef](#)]
130. Patarin, J.; Souldard, M.; Kessler, H.; Guth, J.-L.; Baron, J. Characterization of siliceous MFI-type zeolites containing tetra-, tri-, and dipropylammonium fluoride species. *Zeolites* **1989**, *9*, 397–404. [[CrossRef](#)]

131. Suzuki, K.; Kiyozumi, Y.; Shin, S.; Fujisawa, K.; Watanabe, H.; Saito, K.; Noguchi, K. Zeolite synthesis in the system pyrrolidine- $\text{Na}_2\text{O}-\text{Al}_2\text{O}_3-\text{SiO}_2-\text{H}_2\text{O}$ . *Zeolites* **1986**, *6*, 290–298. [[CrossRef](#)]
132. Crea, F.; Nastro, A.; Nagy, J.; Aiello, R. Synthesis of silicalite 1 from systems with different TPABr/ $\text{SiO}_2$  ratios. *Zeolites* **1988**, *8*, 262–267. [[CrossRef](#)]
133. Ahmed, S.; El-Faer, M.Z.; Abdillahi, M.M.; Siddiqui, M.A.; Barri, S.A. Investigation of the rapid crystallization method for the synthesis of MFI-type zeolites and study of the physicochemical properties of the products. *Zeolites* **1996**, *17*, 373–380. [[CrossRef](#)]
134. Ferchiche, S.; Valcheva-Traykova, M.; Vaughan, D.E.; Warzywoda, J.; Sacco, A. Synthesis of large single crystals of templated Y faujasite. *J. Cryst. Growth* **2001**, *222*, 801–805. [[CrossRef](#)]
135. Mintova, S.; Grand, J.; Valtchev, V. Nanosized zeolites: Quo Vadis? *Comptes Rendus. Chim.* **2016**, *19*, 183–191. [[CrossRef](#)]
136. Mintova, S.; Gilson, J.-P.; Valtchev, V. Advances in nanosized zeolites. *Nanoscale* **2013**, *5*, 6693–6703. [[CrossRef](#)] [[PubMed](#)]
137. Alipour, S.M.; Halladj, R.; Askari, S. Effects of the different synthetic parameters on the crystallinity and crystal size of nanosized ZSM-5 zeolite. *Rev. Chem. Eng.* **2014**, *30*, 289–322. [[CrossRef](#)]